Effect of Swelling Pretreatment on the Deposition Structure on Electroless Copper of Polyacrylonitrile Nanocomposites for Electromagnetic Interference Shielding

Chang-Cheng Chen, Chih-Wei Hung, Sung-Yeng Yang, Chi-Yuan Huang

Department of Materials Engineering, Tatung University, Taipei 104, Taiwan

Received 15 June 2007; accepted 31 March 2008
DOI 10.1002/app.28463
Published online 4 June 2008 in Wiley InterScience (www.interscience.wiley.com).

ABSTRACT: In this investigation, the electroless copper method with various cupric sulfate concentrations (0.24, 0.36, 0.48, 0.60*M*) without sensitizing and activating is used to deposit electroless copper compounds (CuS) on the swelling pretreatment polyacrylonitrile(SPAN) surface for electromagnetic interference (EMI) shielding materials. The acetic acid can swell polyacrylonitrile (PAN) effectively which donot destroy the hexagonal structure of polyacrylonitrile, only looses the molecule chain of polyacrylonitrile then the hexagonal CuS crystal deposits on the SPAN easily, and increases the EMI shielding effectiveness (SE) of CuS-SPAN composites. However, the nearly amorphous of CuS deposits on the surface of without swelling pretreatment PAN(CuS-PAN). The EMI SE of CuS-SPAN composites are better than those of CuS-PAN, 10–15 dB larger from CuS-PAN. In the study, the best EMI SE of CuS-SPAN and CuS-PAN composites are about 30–35 dB and 18–20 dB respectively, as the cupric ion concentration is 0.48*M*. From the high resolution transmission electron micrographs(HR-TEM) analysis, there are two structures, face-centered cubic(FCC) $Cu_{2-x}S$ crystal in the inner layer of CuS-SPAN composite and hexagonal CuS crystal on the outer layer of CuS-SPAN composite, in the SPAN as the cupric ion concentration is 0.48*M*. The particle size distribution of $Cu_{2-x}S$ in the inner layer of CuS-SPAN is from 6 to 30 nm. However, the major particle size distribution of $Cu_{2-x}S$ in the inner layer of CuS-SPAN is from 15 to 20 nm. © 2008 Wiley Periodicals, Inc. J Appl Polym Sci 109: 3679–3688, 2008

Key words: coatings; crystal structure; swelling; nanocomposites; electromagnetic interference (EMI)

INTRODUCTION

Plastics have many advantages, such as lightness of weight, low cost, easy construction of complex shapes, and superior design capabilities. Therefore, plastics have widely been applied to electrical equipment housings, and consumer electronic appliances are usually housed in plastic packaging. Nevertheless, Plastics do not prevent the transmission of electromagnetic waves. Electronic equipment has needed shielding to reduce interference that might abnormally affect their operation and to ensure reliable operation in an electromagnetically polluted environment. In the past, metals were applied to electromagnetic interference (EMI) shielding since they could reflect or conduct the free electrons.[1–3] However, the development of electronic equipment tends to small and lightness of weight in last years. Many technologies have been developed to provide EMI shielding. The techniques for plastic EMI shielding include intrinsic conductive polymers (ICPs),[4] electroplating,[5] electroless plating,[6] conductive paints,[5] metal fillers injected during the molding stage,[7] and other metallization process. Among them, electroless metal plating is probably a preferred way to produce metallization of polymer substrates. This method is based on the chemical reduction of metal ions in the solution to metallic atoms on the surface through a reducing agent in the solution, and is not constrained by the shape, size or conductivity of the supporting substrate.[8] The most widely used metals are copper, silver, and nickel. As electroless method has advantages in terms of coherent metal deposition, excellent conductivity, EMI shielding effectiveness and applicability to complicated shaped substrates.

Ebert[9] indicated that swelling of the membrane material strongly affects solute rejection: dense membranes get narrower pores when swollen. Then, swelling treatment can increase with the molecule chain length and loose between the molecule chain spaces.[10,11] The molecule chain of SPAN during swelling pretreatment possessed loosed and the cupric ion easily penetrated into the SPAN molecule

Correspondence to: C.-Y. Huang (cyhuang@ttu.edu.tw).
Contract grant sponsor: National Science Council; contract grant number: NSC 93-2216-E-036-004.

chain in the electroless copper bath. So, the conductive copper sulfide could deposit into PAN substrate. Copper sulfides exist in a wide variety of compositions, ranging from copper-rich chalcocite (Cu_2S) to copper-deficient villamaninite (CuS_2) with other intermediate compounds, in-between, such as covellite (CuS), djurleite ($Cu_{1.95}S$), and anilite ($Cu_{1.75}S$), among others.[12] Copper sulfides with various stoichiometries are important *p*-type semiconductors and have been extensively used in solar cells.[13,14]

In this article, the acetic acid is used to swell and loose the molecule chain of polyacrylonitrile. And then, various cupric concentrations electroless copper bath are used to deposit copper-sulfide compound on the SPAN film to increase the EMI SE of composites. The FCC $Cu_{2-x}S$ crystal deposits in the inner layer of CuS-SPAN and hexagonal CuS crystal deposits on the outer layer of CuS-PAN.

EXPERIMENTAL

Materials

Polyacrylontrile powders were obtained from Tong Hwa Synthetic and used as the substrate. The particles size of PAN powder is 1–10 μm, and has 93% of polyacrylontrile and (7%) vinyl acetate. The PAN powders were dissolved completely in dimethyformanide (DMF) to form PAN solution. And then, pour the above PAN solution into the petridish slowly. First, it was dried to form the PAN film in oven at 40°C. Second, to make the residual solvent in the PAN film was vaporized, the film was dried in vacuum oven.

Swelling pretreatment

In this investigation, there were three solvents (phosphoric acid, acetic acid and dimethyformanide) for swelling the PAN film (SPAN) and the concentration of solvents were 50 vol % at 25°C for 30 min. After swelling, it was found that the SPAN of acetic acid (99.7%, NIHON SHIYAKU INDUSTRIES Ltd.) had maximum swelling efficient. The result of degree of swelling of SPAN was listed in Table I. Degree of Swelling was measured by the following equation.

TABLE I
The Degree of Swelling of PAN Film in Different Solvents

Solvent	Q
Phosphoric acid	1.38%
Acetic acid	2.20%
Dimethyformanide	1.32%

TABLE II
Composition and Operating Conditions of Electroless Copper Bath

	Concentrations (M)			
Components	Electroless copper bath			
$CuSO_4 \cdot 5H_2O$	0.24	0.36	0.48	0.60
$Na_2S_2O_3 \cdot 5H_2O$	0.12	0.18	0.24	0.30
$NaHSO_3$	0.12	0.18	0.24	0.30
Temperature	95°C			
Time	1 h			
pH	1–2			

$$Q = \{(W_s - W_d)/W_d\} \times 100\%$$

Q: the degree of swelling; W_s: the weight of swelling SPAN film; W_d: the weight of dry PAN film.

Electroless deposit

For composition and operation conditions of electroless copper bath, chemical composition of electroless copper bath are listed in Table II. The cupric sulfate ($CuSO_4 \cdot 5H_2O$), sodium thiosulfate($Na_2S_2O_3 \cdot 5H_2O$) and sodium hydrogen sulfate($NaHSO_3$) were produced by NIHON SHIYAKU INDUSTRIES Ltd. All the specimens were plated in the elecroless copper solution at 95°C for 1 h and were stirred by nitrogen. After plating, the CuS-PAN and CuS-SPAN were washed with water until the surface clean up and then dried in the vacuum oven. The abbreviations of composites are shown in Table III.

EMI SE and resistivity measurement

The shielding effectiveness of the composite was measured by the method using the flanged circular coaxial transmission line holder. The range of frequencies measured in this equipment is from 1 MHz to 1.8 GHz.[15] This holder is similar to that of the circular coaxial transmission line holder. The dynamic rang of EMI SE was 90–100 dBm. The SE values of

TABLE III
Abbreviations of Composites

Sample	PAN un-swelling	PAN swelling	Cupric ion concentration (M)
PAN	•		0
SPAN		•	0
N Series			
N024	•		0.24
N036	•		0.36
N048	•		0.48
N060	•		0.60
S Series			
S024		•	0.24
S036		•	0.36
S048		•	0.48
S060		•	0.60

composites were obtained by taking out the background shielding measurement. However, the measurement frequency range list on ASTM D4935-99 is from 30 MHz to 1.5 GHz. And, the EMI SE is voltage dependent below the range of 30 MHz,[16] the testing frequency range of composites for EMI SE in this investigation is from 30 MHz to 1.5 GHz.[17] The volume electrical resistivity of copper-sulfide PAN composite was detected by HIOKI 3227 megohmmeter. The measurement used a pair of copper clamping apparatus, the distance of clamping apparatus is 1 cm, the range of voltage is 9 V (lower limit value) to 900 V (upper limit value) and the charge time was 20 s. The thickness of CuS-SPAN and CuS-PAN composites were measured by micrometer screw gauge (Mitutoyo MDC-25P), and the thickness range of sample were 0.050–0.085 mm.

Field emission scanning electron microscope imaging

The surface morphology and energy dispersive spectrometer(EDS) of copper-sulfide PAN composites were analyzed by field emission scanning electron microscope(FE-SEM JEOL JSM-6700F), the specimens were coated with platinum for 20 s. The surface and cross section morphology of specimens were viewed by FE-SEM at voltage 1.5 and 3 kV, respectively.

High resolution transmission electron microscopy imaging

The specimens were cross section of composites which were held by silicon chip. Then, the specimens were embedded in epoxy resin and sectioned by ion beam milling (BAL-TEC RES010). By high resolution transmission electron microscopy (HR-TEM, JEM-2010 with AHR) equipment with EDX system was used to analyze the composites and the accelerating voltage was 200 kV.

X-ray diffraction analysis

The X-ray Diffraction Pattern of Cu_xS_y depositions were analyzed at room temperature by X-ray powder diffractometer (XRPD, Japan MAC Sience, MXP18) utilizing Cu Kα radiation of wavelength 0.154 nm. The scanning speed and sample width were 4.0 deg/min and 0.02°, respectively, the scanning range were from 10° to 80°. The composition and structure of the electroless deposition are determined by the conventional 2θ Bragg diffraction method.

RESULTS AND DISCUSSION

In this study, the swelling pretreatment of electroless copper plating affect the structure, morphology and

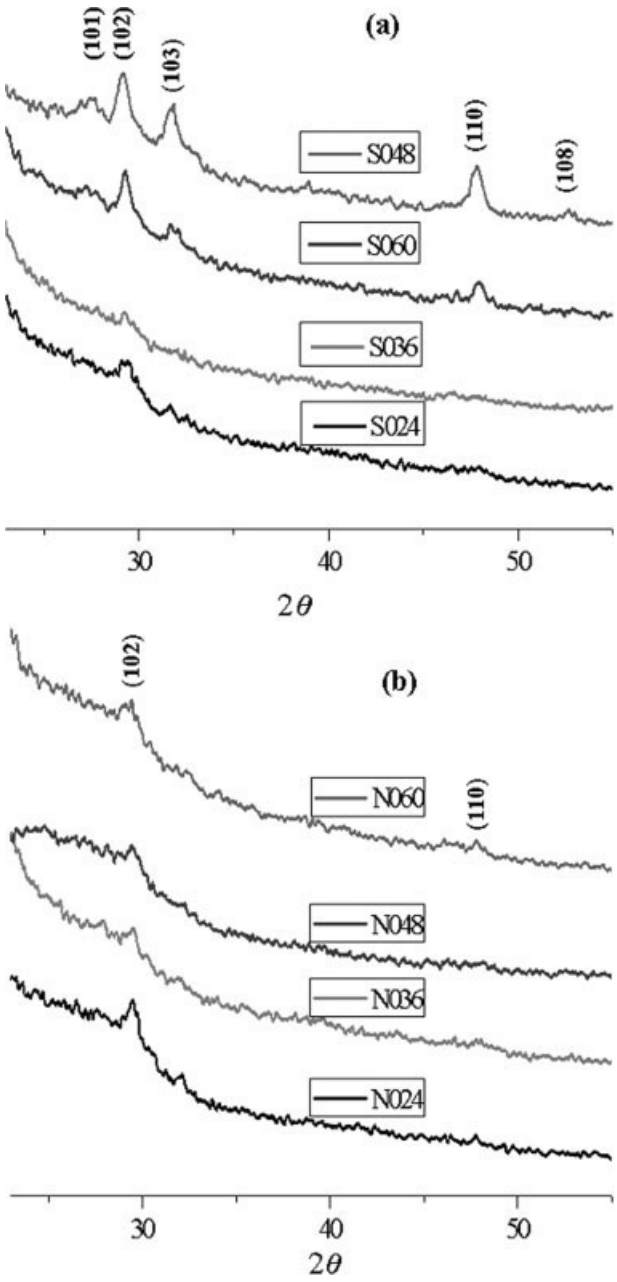

Figure 1 The GIA-XRD diffraction patterns of (a) CuS-PAN and (b) CuS-SPAN.

EMI SE of the composites. The conductive copper-sulfide compound deposition coats on the surface of substrate, the copper-sulfide PAN composite has a good conductivity property.[18–20]

X-ray diffraction and TEM

The X-ray diffraction pattern is used to check out the composition and the structure of copper-sulfur deposition. Because PAN substrate diffraction pattern affect the analysis of Cu_xS_y deposition, grazing incident angle X-ray diffraction (GIA-XRD) analysis

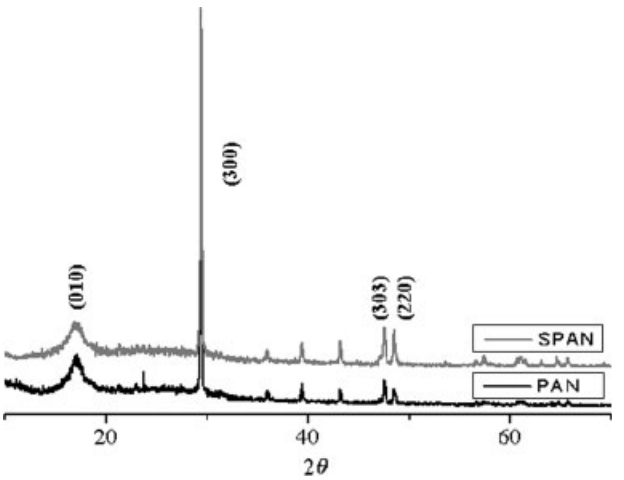

Figure 2 The XRD diffraction patterns of PAN and SPAN film.

can avoid the influence of PAN substrate diffraction pattern. The X-ray diffraction patterns of electroless copper plating depositions are shown in Figure 1. The plating depositions XRD pattern of S series composites show (102), (110), (103), (101), and (108) characteristic peaks of hexagonal CuS(covellite) from JCPDS files No. 06-0464 in Figure 1(a). Without swelling pretreatment, the N series depositions only show weak (102) and (110) characteristic peaks in Figure 1(b), so the depositions are nearly amorphous CuS. Thus, the swelling pretreatment could make the hexagonal CuS crystal deposit onto SPAN film (S series), but the nearly amorphous CuS deposition plat on the PAN film (N series).

Grozdanov et al.[21,22] deposited four kinds of copper-sulfide films, Cu_2S, $Cu_{1.8}S$, $Cu_{1.4}S$, and CuS by electroless chemical plating. The form of CuS (covellite) is thin platy hexagonal crystal, the copper and sulfur ions in the covellite are tetrahedrons structure.[12] The copper ion is at the center combined with three sulfur ions in triangular groups on their bases form sheets, these triangular groups lie in a plane between the tetragonal sheets.[12,23] In this study, the CuS deposits on the PAN substrate, and the possible reaction mechanism was shown in following equations:

$$Cu^{2+} + S_2O_3^{2-} \longrightarrow Cu_2S_2O_3 \downarrow$$

$$Cu_2S_2O_3 + H_2O \longrightarrow CuS \downarrow + SO_4^{2-} + 2H^+$$

Klement et al.[24] and Allen et al.[25] indicated that the syndiotactic PAN formed hexagonal and orthorhombic structure, and the isotactic PAN formed tetrahedral unit cell. The structure of covellite is also hexagonal according to the JCPDS files 06-0464. Figure 2 shows that the PAN and SPAN also possessed hexagonal structure, and the characteristic peaks of PAN do not shift during swelling treatment. The swelling pretreatment which does not destroy the hexagonal structure of SPAN, only looses the molecule chain of SPAN. Therefore, the hexagonal structure of CuS is easily to deposit onto the SPAN film. On the other hand, the SPAN possessed looses molecule chain structure, the cupric and sulfurate ion easily penetrate into the SPAN molecule chain in the electroless copper bath. Thus, the swelling pretreatment makes for the hexagonal CuS crystal deposit onto SPAN film easily.

The interaction mechanism between Cu^{2+} and SPAN are shown in Figure 3. Acrylonitrile group (—C≡N) possesses very high polarity. This arises from the strong dipole moment of the nitrile groups. The lone pair orbital of nitrogen can engage in hydrogen bonding and electros in the π orbital of the nitrile triple bond which can interact with transition metal ions.[26] That is the reason the electroless copper method without sensitizing and activating in this study.

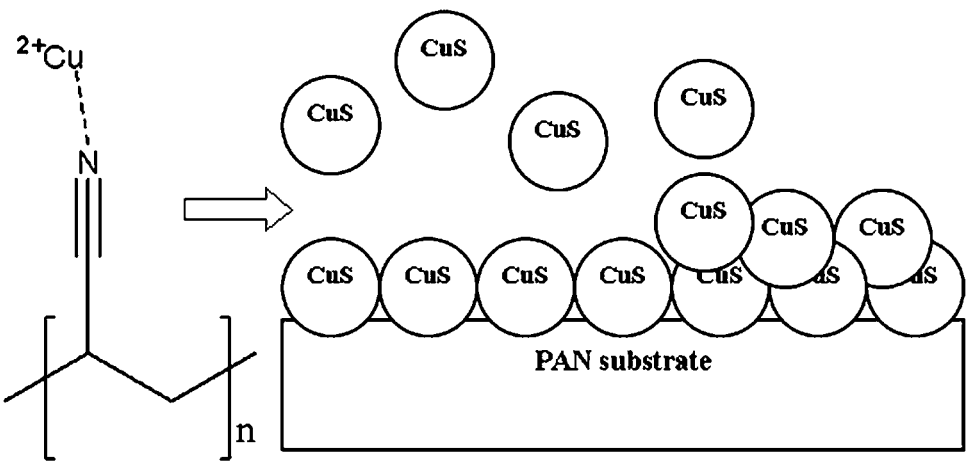

Figure 3 The deposition mechanism between CuS and PAN.

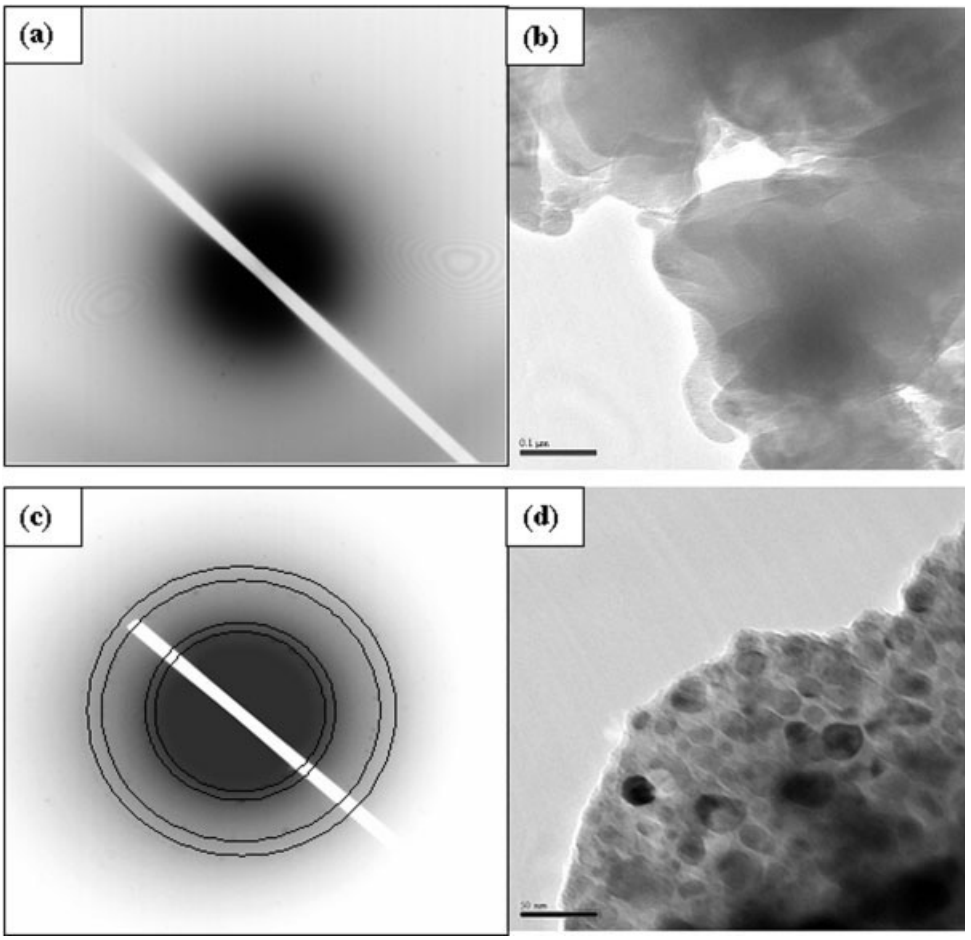

Figure 4 HR-TEM of inner cross section morphology of N048 (a) SAD; (b) bright image and S048 (c) SAD; (d) bright image.

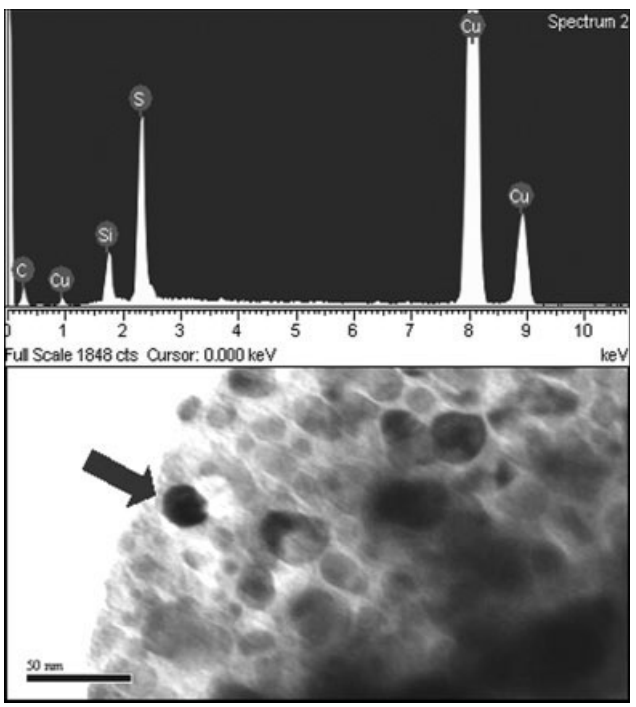

Figure 5 HR-TEM bright image of cross section morphology and EDX spectrum (S048) in the inner CuS-SPAN composites.

High resolution transmission electron micrographs (HR-TEM) bright image of the inner cross section morphology and select area diffraction (SAD) pattern of CuS-PAN (N048) and CuS-SPAN (S048) composites are shown in Figure 4. The SAD pattern in Figure 4(a) identifies that the SAD pattern of specimen does not have any diffusion halo rings existence,

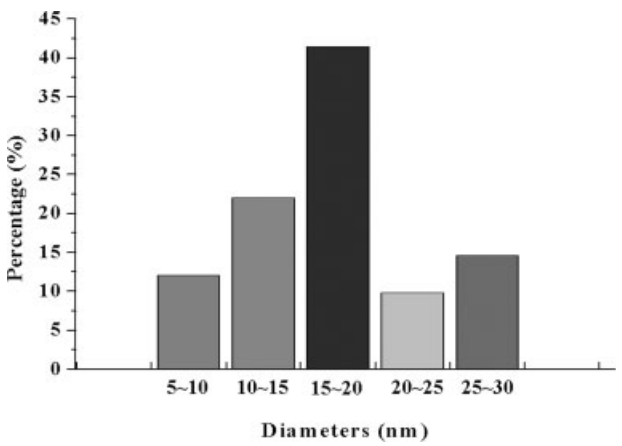

Figure 6 Diameter distributions of $Cu_{2-x}S$ nano-particles.

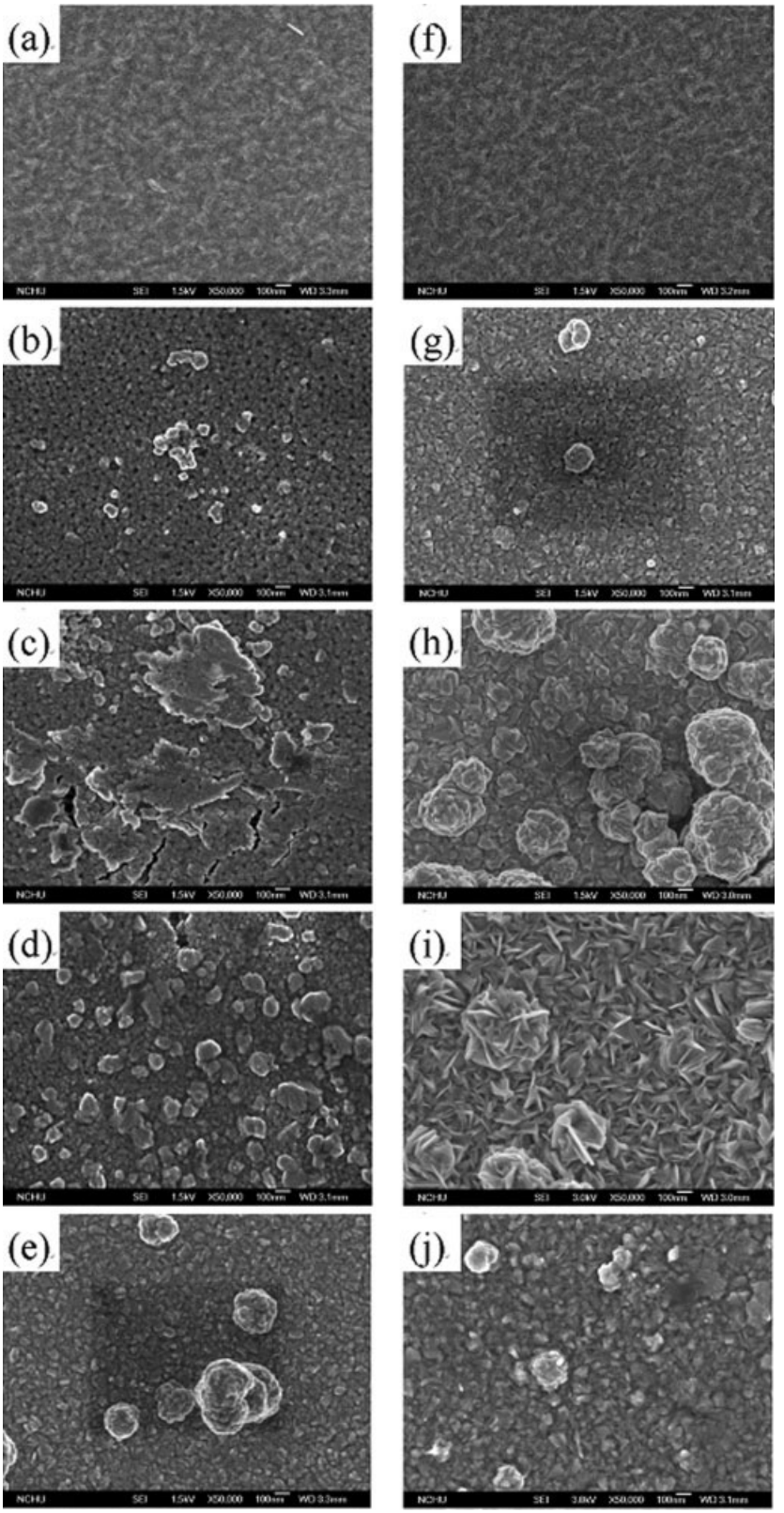

Figure 7 FE-SEM surface morphologies of CuS-PAN and CuS-SPAN at various cupric ion concentrations as follow: (a) PAN, (b) N024, (c) N036, (d) N048, (e) N060, (f) SPAN, (g) S024, (h) S036, (i) S048, (j) S060.

and without any copper-sulfide compound particles in the bright image [Fig. 4(b)]. This indicates that without any CuS is deposited in the inner layer of PAN. Figure 4(a,b) prove that the amorphous CuS particles donot diffuse into the inner PAN substrate without swelling pretreatment. However, we observe

four Debye-Scherrer rings from the SAD pattern of CuS-SPAN composite in Figure 4(c). Those diffraction patterns correspond to a FCC image structure which coincides with that of Valova et al.[27] described. According to the diffraction pattern, the formula of inner CuS-SPAN composite is $Cu_{2-x}S$ crystal (JCPDS files NO. 02-1281). Zhu et al.[28] also indicated that the product of CuS (covellite) crystal included the peak of $Cu_{2-x}S$ phase by XRD analysis. It is interesting that the $Cu_{2-x}S$ in the inner CuS-SPAN(S048) is face-center cubic(FCC) structure and the CuS crystal deposition outer CuS-SPAN(S048) is hexagonal structure. The reason causes the different structure from inner and outer of CuS-SPAN(S048) composites should be further study in the future.

EDX spectrum shows the cross section morphology of S048 by HR-TEM (Fig. 5). Figure 5 shows that the copper and sulfide element are detected in the S048. The particles of $Cu_{2-x}S$ compound with various diameter size and ball-like shape can be seen in the inner CuS-SPAN composite. The particle size distribution of $Cu_{2-x}S$ in the inner layer of CuS-SPAN is from 6 to 30 nm. However, the major particle size distribution of $Cu_{2-x}S$ in the inner layer of CuS-SPAN is from 15 to 20 nm. The measurement result is concluding in the Figure 6.

As the result, the hexagonal CuS crystal deposits on the surface of SPAN and the amorphous CuS plats on surface of the PAN. However, as the cupric ion concentration is 0.48*M*, the FCC crystal $Cu_{2-x}S$ is deposited in the inner CuS-SPAN composite.

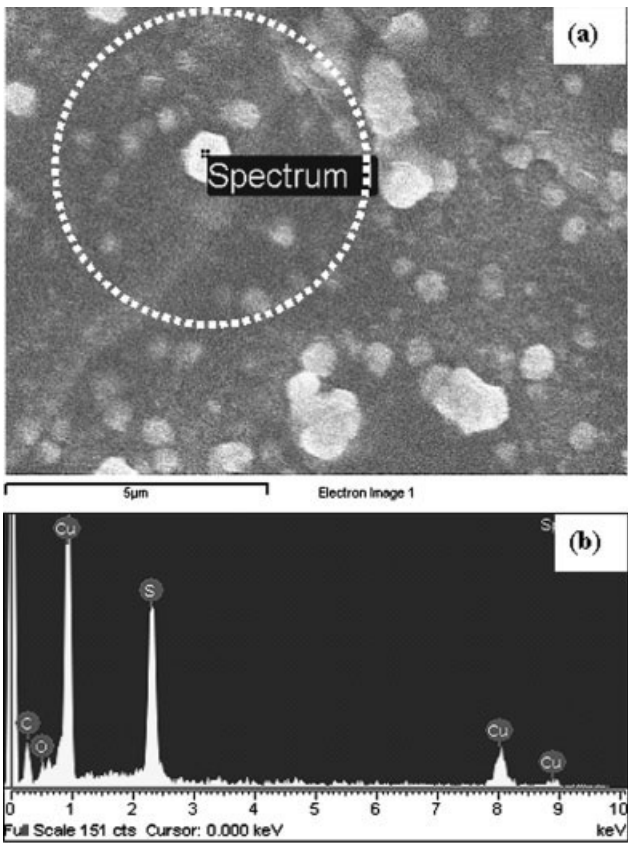

Figure 8 Element analysis of S048 by EDS.

Surface morphology and element analysis

Figure 7 shows the morphology of CuS-PAN and CuS-SPAN with the different cupric ion concentration by Field Emission Scanning Electron Microscope. The smooth surface of PAN and SPAN film show in Figure 7(a,f), respectively. Figure 7(b,e,g,j) indicate that the CuS particles form a regular and continuous base on the film surface. Moreover, a few of un-regular particle produce on the base. From the Figure 7(b,g), the deposition layer on the SPAN [Fig. 7(g)] is more dense than that on the PAN [Fig. 7(b)]. In Figure 7(c,d,h), they show some growing regions of agglomerates over the previous layer, and the agglomerates particles form the slice [Fig. 7(c)] and ball [Fig. 7(h)] shapes. Figure 7(i) (S048) displays a continuous base of flake grains. From the GIA-XRD analysis [Fig. 1(a)], the S048 shows the stronger characteristic peaks of hexagonal CuS. Lindroos et al.[29] and Zhang et al.[30] also indicated that the flake grains shapes were hexagonal CuS (covellite) structure. In this study, the hexagonal CuS deposition shows crystal structure as the cupric concentration is 0.48*M* with swelling pretreatment. In Figure 7, when the cupric concentrations is between 0.24 and 0.48*M*, the CuS particle sizes of CuS-SPAN are lager than those of CuS-PAN, and the particle size of CuS increase with increasing cupric concentration. However, when the cupric concentration up to 0.60*M*, the particle size of CuS decrease with increasing cupric concentration. It is suggested that the reaction rate is too fast to grow CuS on the surface of substrate.

The EDS analysis of S048 shows in Figure 8, and the scanning range is about a circle of diameter 5 µm [Fig. 8(a)]. It is observed that amount of copper and sulfur element exist in the plating deposition. It further more confirms that the electroless plating deposition is copper-sulfur compound.

The FESEM micrography of cross section morphology of CuS-PAN and CuS-SPAN composites are shown in Figure 9. It is observed that the deposition thickness of CuS-SPAN composites are higher than those of CuS-PAN, besides the cupric concentration is 0.60*M*. The deposition thickness of N060 [Fig. 9(e)] and S060 [Fig. 9(j)] are almost the same. Among of various composites, S048 [Fig. 9(i)] possesses the thickest CuS deposition (240 nm), it is higher about two times than the deposition thickness of other composites. In Figure 9(c–e), there are some holes between CuS deposition and PAN (arrowhead). However, there is no hole existence between CuS

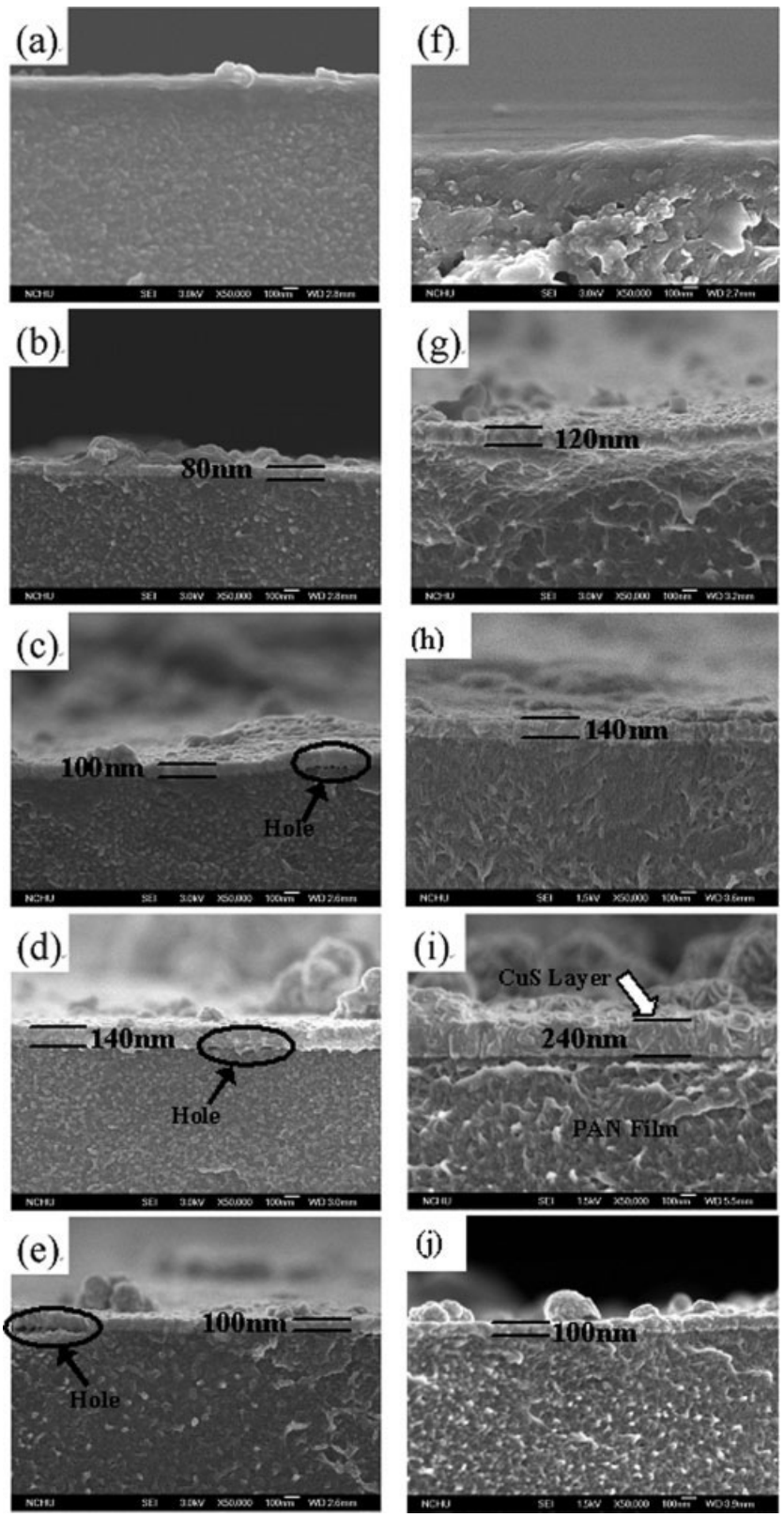

Figure 9 FE-SEM cross-section morphologies of CuS-PAN and CuS-SPAN at various cupric ion concentrations as follow: (a) PAN, (b) N024, (c) N036, (d) N048, (e) N060, (f) SPAN, (g) S024, (h) S036, (i) S048, (j) S060.

deposition and SPAN. During swelling pretreatment, the cupric and sulfurate ion diffuse into the molecular chain of SPAN easily, and the structure of SPAN and CuS own the same hexagonal structure. Therefore, the swelling pretreatment can improve the interface of CuS deposition and SPAN, and the

hexagonal CuS deposition grows from the inner to surface of SPAN film. The CuS thickness of S series composites are thicker than those of N series composites.

EMI shielding effectiveness and resistivity analysis

The EMI SE of the N series and S series composites are shown in Figure 10. This figure [Fig. 10(a)] shows that the EMI SE of N series composites do not markedly increase with increasing cupric ion concentration. The EMI SE of N048 composites is 18–20 dB. Figure 10 shows that the EMI SE of CuS-SPAN composites are better than those of CuS-PAN composites, the EMI SE of S048 composites reaches 30–35 dB, 10–15 dB higher from CuS-PAN (N048). Han et al.[31] indicated that the thickness of conductive layer coating increased and consequently resulted in higher EMI SE. Figure 9 also shows that the S048 possesses the thickest thickness of CuS deposition. Luo et al.[32] also indicated that high conductivity and dielectric constant of materials contribute to high EMI SE. In this investigation, the resistivities of S series composites are lower than those of N series composites, and the resistivity of various composites are shown in Figure 11. Figure 11 shows that S048 possesses the lowest resistivity of all composites. Therefore, S048 shows the best EMI SE of all composites. In addition to S048, the S060 owns the better resistivity than those of others (Fig. 11). However, the EMI SE of N048 and S036 are better than that of S060 (Fig. 10). It is because that the CuS thickness of N048 and S036 are thicker than that of S060. Hence, the affection of deposition thickness is larger than that of resistivity for EMI SE. In this study, the mainly affection factor for EMI SE is deposition thickness.

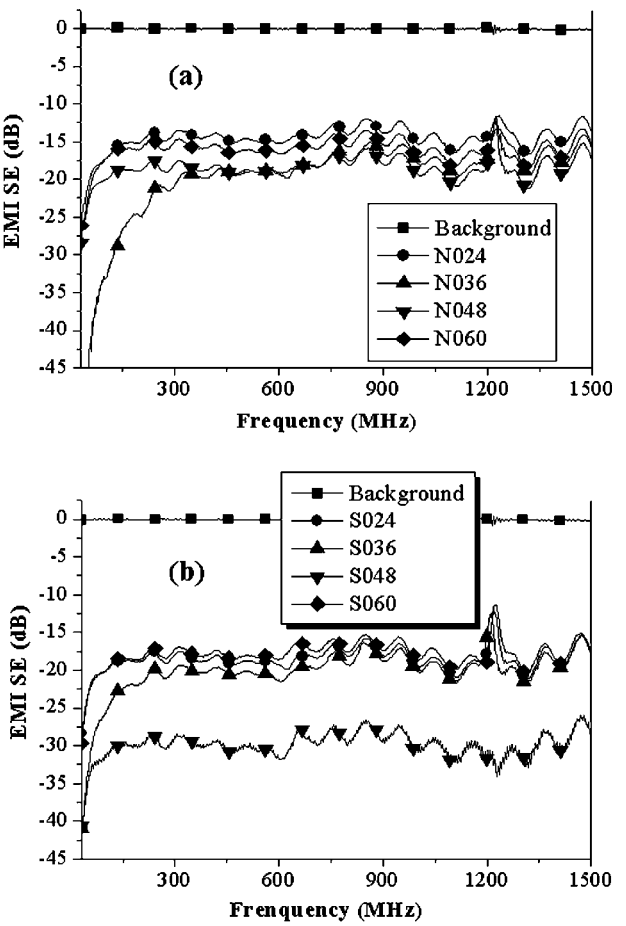

Figure 10 The EMI SE of the (a) CuS-PAN and (b) CuS-SPAN composites.

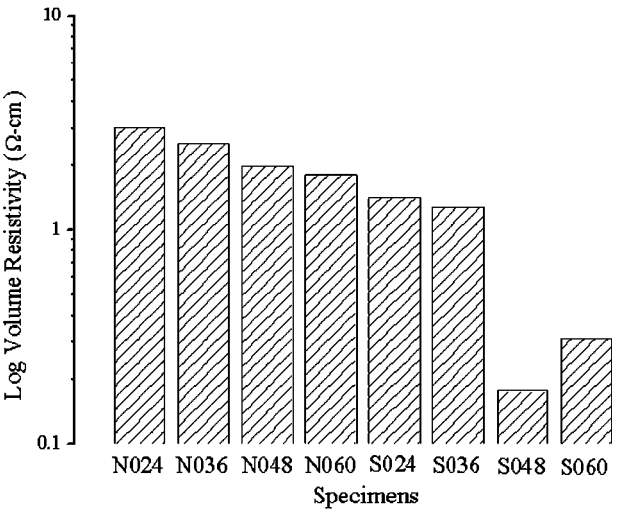

Figure 11 The volume resistivities of CuS-SPAN and CuS-PAN composites.

CONCLUSIONS

The swelling treatment which donot destroy the hexagonal structure of SPAN just only loosed the molecule chain of SPAN. Thus, the cupric and sulfurate ion easily penetrated into the PAN substrate, and the structure of SPAN and CuS own the same hexagonal structure. Therefore, the hexagonal CuS crystal easily deposits on the surface of SPAN. However, the nearly amorphous CuS plats on surface of the PAN. As the cupric ion concentration is 0.48*M*, the FCC crystal $Cu_{2-x}S$ is deposited in the inner CuS-SPAN composite. The particles of $Cu_{2-x}S$ compound with various diameter size and ball-like shape can be seen in the inner CuS-SPAN composite. The particle size distribution of $Cu_{2-x}S$ in the inner layer of CuS-SPAN is from 6 to 30 nm, and the major particle size distribution of $Cu_{2-x}S$ in the inner layer of CuS-SPAN is from 15 to 20 nm. Generally, the EMI SE of S series composites are better than those of N series composites, especially S048, the EMI SE reaches 30–35 dB, 10–15 dB higher from CuS-PAN (N048). In this investigation, the S048 possesses the best EMI SE of all composites. It is

because that the mainly affection factor for EMI SE is deposition thickness in this study, and the 240 nm CuS thickness of S048 is higher about two times than that of other composites. Therefore, S048 shows advantaged EMI SE of all composites. With swelling pretreatment and appropriate cupric ion concentration(0.48*M*), the thick and crystalline CuS deposition is plated on the SPAN and increases about 50–75% EMI SE.

Tong-Hwa Synthetic Fiber Co., Ltd kindly supplied to Polyacrylonitrile (PAN) powder.

References

1. Huang, C. Y.; Mo, W. W. J Appl Polym Sci 2002, 85, 1661.
2. Chen, S. C.; Chien, R. D.; Lee, P. H.; Huang, J. S. J Appl Polym Sci 2005, 98, 1072.
3. Huang, C. Y.; Mo, W. W.; Roan, M. L. Surf Coat Technol 2004, 184, 163.
4. Kim, S. H.; Jang, S. H.; Byun, S. W.; Lee, J. Y.; Joo, J. S.; Jeong, S. H.; Park, M. J. J Appl Polym Sci 2003, 87, 1969.
5. Huang, J. C. Adv Polym Tech 1995, 14, 137.
6. Oh, K. W.; Kim, D. J.; Kim, S. H. J Appl Polym Sci 2002, 84, 1369.
7. Chou, K. S.; Huang, K. C.; Shih, Z. H. J Appl Polym Sci 2005, 97, 128.
8. Lin, Y. M.; Yen, S. C. Appl Surf Sci 2001, 178, 116.
9. Ebert, K. Presented at NMG Symposium, Ede, The Netherlands, June 11, 2002.
10. Geens, J.; Van der Bruggen, B.; Vandecasteele, C. Chem Eng Sci 2004, 59, 1161.
11. Christopher, S. B.; Nikolaos, A. P. Biomaterials 1999, 20, 721.
12. Tezuka, K.; Sheets, W. C.; Kurihara, R.; Shan, Y. J.; Imoto, H.; Marks, T. J.; Poeppelmeier, K. R. Solid State Sci 2007, 9, 95.
13. Xu, C.; Zhang, Z.; Ye, Q.; Liu, X. Chem Lett 2003, 32, 198.
14. Zhang, Y.; Qiao, Z.; Chen, X. J Mater Chem 2002, 12, 2747.
15. Wilson, P. F.; Ma, M. T. IEEE Trans Electromagn Compact 1998, 30, 239.
16. Arnold, W. M.; Harris, P.; Partridge, C. A.; Andrews, M. K. IEEE Annu Report—Conference on Electrical Insulation and Dielectric Phenomena, San Francisco, 1996.
17. Huang, C. Y.; Mo, W. W. Surf Coat Technol 2002, 154, 55.
18. Baseri, S.; Zadhoush, A.; Morshed, M.; Amirnasr, M.; Azarnasab, M. J Appl Polym Sci 2007, 104, 2579.
19. Im, S. S.; Lee, J. S.; Kang, E. Y. J Appl Polym Sci 1992, 45, 827.
20. Im, S. S.; Im, H. S.; Kang, E. Y. J Appl Polym Sci 1990, 41, 1517.
21. Grozdanov, I.; Najdoski, M. J Solid State Chem 1995, 114, 469.
22. Grozdanov, I. Appl Surf Sci 1995, 84, 325.
23. Berry L. G. Am Mineralogist 1954, 39, 504.
24. Klement, J. J.; Geil, P. H. J Polym Sci A-2: Polym Phys 1968, 6, 1381.
25. Allen, R. A.; Ward, I. M. Polymer 1994, 35, 2063.
26. Henrici-Olive, G.; Olive, S.; Adv Polym Sci 1979, 32, 125.
27. Valova, E.; Dille, J.; Armyanov, S.; Georgieva, J.; Tatchev, D.; Marinov, M.; Delpancke, J. L.; Steenhaut, O.; Hubin, A. Surf Coat Technol 2005, 190, 336.
28. Zhu, H.; Ji, X.; Yang, D.; Ji, Y.; Zhang, H. Microporous Mesoporous Mater 2005, 80, 153.
29. Lindroos, S.; Arnold, A.; Leskelä, M. Appl Surf Sci 2000, 158, 75.
30. Zhang, H. T.; Wu, G.; Chen, X. H. Mater Chem Phys 2006, 98, 298.
31. Han, E. G.; Kim, E. A.; Oh, K. W. Synth Met 2001, 123, 469.
32. Luo, X. C.; Chung, D. D. L. Compos B 1999, 30, 227.